Response Test of Power Transformer Windings Excited by Nanosecond Pulse

Xinhe Liu*, Wenwu Huang and Haitao Wu

Shenzhen Power Supply Bureau Co. Ltd, Shenzhen 518000, China
E-mail: liuxinhevip@163.com
**Corresponding Author*

Received 15 June 2021; Accepted 11 July 2021;
Publication 27 August 2021

Abstract

At present, the detection of transformer winding deformation in the offline phase, in order to discover the small transformer winding deformation, realize the online monitoring, in this paper, using nanosecond pulse frequency response analysis method, the detection of transformer winding deformation is studied, the results show that the nanosecond pulse frequency response analysis method in the detection of transformer winding deformation with high reliability and sensitivity.In order to verify the repeatability of the method, the method was used again at a 30-day interval under the condition that the detection environment was basically unchanged. The ρ value was 0.9719 in the range of 1 kHz$\sim$1 MHz.

Keywords: Power transformer, winding deformation, nanosecond pulse, frequency response analysis.

1 Introduction

With the advancement of the economic construction in our country, the power consumption increased year by year, in order to meet the demand, more and

Distributed Generation & Alternative Energy Journal, Vol. 37_1, 103–116.
doi: 10.13052/dgaej2156-3306.3715

more large capacity substation project arises at the historic moment, power transformer manufacturing tend to be large, higher voltage level, the capacity is bigger, more complex, and more expensive, increasing the importance of the safe and stable operation of the transformer, the transformer in the event of failure, In addition, the maintenance time of power transformer usually lasts for about half a year , which brings great economic losses to social production and inconvenience to life.

FRA method is a comparative method, which compares the detected frequency response curve with the reference curve, and the difference between the two indicates a certain form of winding deformation. The FRA method is divided into Sweep Frequency Response Analysis (SFRA) and Impulse Frequency Response Analysis (IFRA). The only difference between the two is the way in which the frequency response curve is obtained. The excitation source of SFRA method is the sweep signal generator, and the whole frequency response curve is obtained by gradually changing the frequency of the excitation signal and tracing points in turn. IFRA is developed on the basis of LVI. The Fast Fourier Transform (FFT) is used to convert the excitation and response signals of the LVI method into the frequency domain respectively, and then the full frequency response curve is obtained at one time. Theoretically, the results of both methods should be the same.

At present, SFRA method is widely used at home and abroad due to its high signal-to-noise ratio, stable experimental results and high repeatability. However, the actual use of IFRA method is less. At present, the FRA method referred to at home and abroad usually refers to SFRA.

This study aims at the application of nanosecond pulse frequency response analysis method in transformer winding deformation detection, and verifies the practicability of the nanosecond pulse frequency response analysis method.

Power transformer is one of the core equipment in power system. It is the hub of power grid and plays the role of interconnection and power exchange of power grid with different voltage levels.Trela et al. discussed the progress in frequency response interpretation of these important equipment in the power grid and established a numerical model to reduce the time required for electromagnetic field analysis of hundreds of turns windings [1]. Ahour et al. established an appropriate mathematical model, which could accurately simulate the transient behavior of windings [2]. In order to reduce the resistance loss caused by the skin effect and proximity effect in the high-frequency induction wireless transmission coil, Zhang et al. established an impedance calculation model for the electromagnetic field and resistance

loss of the double-layer composite conductor in the frequency range below 100 kHz [3]. UHF method is an effective method for partial discharge detection of power transformers. The characteristic parameters extracted from UHF PD signal can be used to identify the types of insulation defects. Wenjun et al. proposed a time-frequency feature parameter extraction method based on texture features [4].

Transformer fault detection is an important and difficult task that has not been solved yet. It is well known that the most sensitive and promising method is the nanosecond low voltage pulse test. Xiao et al. designed a deformation test scheme for the nanosecond pulse winding of 220kV fault transformer [5]. Devies et al. designed a push-pull nanosecond pulse generator based on power MOSFET [6]. Zhang et al. proposed a nanosecond pulse frequency response method [7] in order to realize online detection of power transformer winding deformation faults. In order to realize online detection of transformer winding deformation, overcome the shortcomings of offline detection and discover potential transformer faults, Ding et al. proposed a method of live detection of transformer winding micro-deformation based on nanosecond impulse response analysis [8]. Kovrigin et al. studied a response waveform processing method based on nanosecond low-voltage pulse to diagnose the internal physical state of power transformer windings [9]. Bai optimized the power measurement strategy of nanosecond pulse coaxial DBDS, and studied the effects of different experimental parameters on plasma energy deposition and reduction electric field [10].

2 Research Methods

2.1 Experimental Transformer

The experimental transformer is a three-coherent distribution transformer with rated capacity of 50 kVA and rated voltage of 10/0.4 kV. The high voltage side is a continuous winding with 60 pieces of 25 turns for each piece, while the low voltage side is a cylindrical winding with 60 turns in total. The high and low voltage side windings are all star connected. Other parameters are shown in Table 1. The experiment in this paper is only carried out for A-phase. The neutral points of the high and low voltage side windings are grounded, and the rest of the unrelated uniform terminals float to the ground.

This transformer is a customized transformer for the experiment. The 15-cake coil at the top of the high-voltage side winding of each phase can be moved longitudinally as a whole. By inserting a plastic insulating partition

Table 1 Transformer parameters to be measured

Brand: Suntec Electric	Type: SG10-50/10/0.4 Dry Type Power Transformer
Nominal capacity: 50 kVA	Rated frequency: 50 Hz
Rated voltage of primary side: 10 kV	Rated voltage of secondary side: 400 V
Primary side rated current: 2.887 A	Secondary side rated current: 72.2 A
Short-circuit impedance (%, converted to primary side): 4.1	The high voltage winding is 60 pancakes, each pancake is 23 turns.
The phase number: 3	Insulation class: F
Standard: GB1094.11 IEC60076-11	The manufacturing date: In December 2013
Link category: Yyn	

between the 15th cake and the 16th cake, the longitudinal interval between the movable part at the upper part of the winding and the fixed part at the lower part can be changed, thus simulating the axial displacement fault of the winding.The thickness of each insulating board is 10 mm, and a total of 3 layers can be added. If it is assumed that the winding is in normal state when there is no insulating board, a total of three degrees of axial displacement faults of the winding can be simulated.

2.2 Impulse Frequency Response Analysis (IFRA)

The maximum pulse in the frequency component of the six pulses in Table 2 is adopted, and pulse 6 is used as the excitation signal, tr = 30 ns, tw = 300 ns, in order to improve the efficiency of data storage and calculation, the maximum sampling rate of 5 GSA/s of oscilloscope is not adopted, I'm going to set fs = 1 GSa/s, Storage depth N = 1 MSa,the number of samples n = 50, in order to reduce the bending and reflection of electromagnetic waves in the system, the oscilloscope input internal resistance is adjusted to 50O, at this time, the oscilloscope port input voltage limit is 5 V. Gradually increase the VPeak during the experiment, and finally set it to 600 V. The denoising of the obtained frequency response curve was performed by wavelet threshold denoising with a frequency resolution of 1kHz and a bandwidth upper limit of 10 MHz.

Set the SFRA detection frequency band and the sampling points of each frequency band. A total of 2000 points are sampled, as shown in Table 3. Except for 10 Hz $\sim$ 100 Hz and 100 Hz $\sim$ 1 kHz, the maximum sampling

Table 2 Pulse waveform parameters

Pulse Number	t_r/ns	t_w/ns
1	$5 \pm 30\%$	$25 \pm 20\%$
2	$5 \pm 30\%$	$50 \pm 20\%$
3	$15 \pm 30\%$	$75 \pm 20\%$
4	$15 \pm 30\%$	$150 \pm 20\%$
5	$30 \pm 30\%$	$150 \pm 20\%$
6	$30 \pm 30\%$	$300 \pm 20\%$

Table 3 Sampling parameters of frequency response analyzer

Spectrum	The Sampling Points	Frequency Resolution
10 Hz∼100 Hz	100	0.9 Hz
100 Hz∼1 kHz	300	3 Hz
1 kHz∼10 kHz	400	22.5 Hz
10 kHz∼100 kHz	400	225 Hz
100 kHz∼1 MHz	400	2.25 kHz
1 MHz∼10 MHz	400	22.5 kHz

points of this frequency sweep analyzer in this frequency band are selected in other frequency bands.

2.3 Experimental Steps

On a dry type distribution transformer to simulate axial displacement fault, three levels of winding respectively built by nanosecond IFRA detection system and a frequency response analyzer, measuring of the transformer under normal and failure extent of the frequency response curve, compared two kinds of methods to verify income curve similarity nanosecond IFRA method, the reliability of the results, The sensitivity of the nanosecond IFRA method was verified by comparing the trend of frequency response curve with increasing fault severity under the two methods. The wiring mode has an influence on the frequency response detection results. Therefore, the reliability and sensitivity verification experiments were carried out in EE and II wiring modes respectively. (In the IEC standard for detection of FRA transformer winding deformation, four recommended wiring modes are given. The two commonly used wiring methods are EE (end-to-end Measurement) and II(Inductive inter-winding Measurement). In order to verify the repeatability

of the nanosecond IFRA method, the test was carried out again at a 30-day interval under the experimental environment basically unchanged, and the results were compared with those of the first day. The correlation coefficient ρ and Euclidean distance ed were introduced to quantitatively analyze the similarity of the curves.

3 Results Analysis and Discussion

3.1 Reliability Verification of Nanosecond IFRA Method

Normal windings are tested by SFRA and nanosecond IFRA. By comparing the two methods, it can be seen that within the range of less than 4 MHz, the consistency of the two methods is relatively high. Under EE and II wiring modes, the resonant point positions of the detection results of the two methods are basically the same, with only a few amplitude differences in the frequency range.Within the range of 4 MHz$\sim$10 MHz, the results of the two methods have relatively large differences, mainly reflected in the amplitude. Only in the EE connection mode, the difference of resonance points appears around 8.2 MHz and 9.6 MHz. It can be concluded that both SFRA method and nanosecond IFRA method have good consistency under EE and II connection modes.The results of the nanosecond IFRA method can be considered reliable.

3.2 Sensitivity Verification of Nanosecond IFRA Method

In EE connection mode, frequency response curves detected by SFRA method and nanosecond IFRA method at different axial displacement fault degrees are obtained; in II connection mode, frequency response curves detected by SFRA method and nanosecond IFRA method at different axial displacement fault degrees are obtained. It can be seen from the curves that,Both the SFRA method and the nanosecond IFRA method can sensitively detect faults at all levels under both EE and II wiring modes, and the curves obtained by the two methods have the same variation trend with the deepening of the fault degree.

In the EE wiring mode, the axial displacement fault of the winding is mainly reflected in the frequency response curve within 1MHz, and the change is small in other frequency bands. In the II wiring mode, the axial displacement fault of the winding is also mainly reflected within 1MHz, but the change in other frequency bands is greater than that in the EE mode.

Table 4 Statistical parameters of measured frequency response curves of nanosecond IFRA system at various fault degrees under EE wiring mode

Parameter	Degree of Fault	1 kHz∼ 1 MHz	1 MHz∼2 MHz	2 MHz∼5 MHz	5 MHz∼10 MHz
ρ	1	**0.9375**	0.9408	0.9925	0.9987
	2	**0.8569**	0.8815	0.9863	0.9985
	3	**0.7959**	0.8351	0.9817	0.9982
ed	1	**2.0063**	0.6518	0.2492	0.1175
	2	**3.0158**	0.9519	0.3383	0.1338
	3	**3.5053**	1.1324	0.3964	0.1361

Table 5 Statistical parameters of measured frequency response curves of nanosecond IFRA system at various fault degrees under II wiring mode

Parameter	Degree of Fault	1 kHz∼1 MHz	1 MHz∼2 MHz	2 MHz∼5 MHz	5 MHz∼10 MHz
ρ	12	**0.9732**	0.9828	0.9864	0.9851
	2	**0.9366**	0.9637	0.9666	0.9780
	3	**0.9123**	0.9542	0.9391	0.9658
ed	12	**1.3162**	0.3868	0.2722	0.1603
	2	**2.4877**	0.7431	0.6409	0.2573
	3	**3.7364**	1.0944	1.0680	0.5405

In EE wiring mode, the oscillation amplitude of the frequency response in the range of 0.8 MHz∼0.9 MHz decreases with the deepening of the fault degree, and with the left shift of the frequency response curve. In II wiring mode, the two resonant points near 0.25 MHz gradually disappear with the deepening of the fault degree. The resonant peak near 0.35 MHz gradually becomes a resonant valley.

Tables 4 and 5 are respectively the ρ and ED of the frequency response curves measured by the nanosecond IFRA method at various fault degrees and the curves at various frequency bands when the windings are normal under EE and II wiring modes. The minimum value of ρ and the maximum value of ED in each row are bolded. According to the transverse analysis, the frequency band where the minimum value of ρ and the maximum value of Ed are the frequency band with the most obvious change in the frequency response curve. As can be seen from the table, only the data in the frequency band of 1 kHz∼1 MHz are bolded under the two wiring modes. It shows that

Table 6 Correlation coefficient of each fault degree of SFRA and fault degree diagnosis under EE wiring mode

The Correlation Coefficient	Frequency Range	Degree of Failure 1	Fault Degree 2	Degree of Failure 3
*R*LF	1 kHZ∼100 kHz	1.6949	2.2682	2.1060
*R*MF	100 kHz∼600 kHz	1.2506	0.9126	0.7127
*R*HF	600 kHz∼1000 kHz	0.8511	0.5819	0.4204
Degree of winding deformation		mild	mild	mild

Table 7 Correlation coefficient of each fault degree of SFRA and fault degree diagnosis under II wiring mode

The Correlation Coefficient	Frequency Range	Degree of Failure 1	Fault Degree 2	Degree of Failure 3
*R*LF	1 kHZ∼100 kHz	3.3899	3.0913	2.8903
*R*MF	100 kHz∼600 kHz	1.0797	0.7433	0.6290
*R*HF	600 kHz∼1000 kHz	0.9261	0.5708	0.4360
Degree of winding deformation		mild	mild	mild

the axial displacement fault simulated in the experiment is mainly reflected in this frequency band of frequency response under EE and II wiring modes. Longitudinal analysis shows that in each frequency band under the two wiring modes, the value of ρ is always gradually decreased and the value of Ed is always gradually increased with the increase of fault degree. This trend of ρ and Ed reflects that the measured frequency response curve is more and more inconsistent with the normal curve with the increase of fault degree. The sensitivity of the nanosecond IFRA method is verified from the perspective of data analysis.

According to the calculation of the frequency response curves measured by the SFRA method under various fault degrees, the correlation coefficients between the three frequency bands of low frequency, middle frequency and high frequency and the winding under normal conditions are obtained. The results are shown in Tables 6 and 7. From the table, it can be seen that the three degrees of winding displacement faults simulated in this study can all be judged as mild winding deformation, and the nanosecond IFRA method can clearly distinguish the three degrees of faults, so it can be considered that this method has good sensitivity.

Table 8 Correlation coefficients of two nanosecond IFRA test results at an interval of 30 days in each frequency band

Parameter	1 kHz∼1 MHz	1 MHz∼2 MHz	2 MHz∼5 MHz	5 MHz∼10 MHz
ρ	0.9719	0.9900	0.9661	0.9479

3.3 Repeatability Verification of Nanosecond IFRA Method

According to the two nanosecond IFRA test results with an interval of 30 days, it can be seen that the consistency of the two test results is high. The Spearman correlation coefficient of the two curves is calculated in Table 8, and it can be seen that the correlation coefficient of the two curves is high in all frequency bands. Through comparison, it can be seen that in the two nanosecond IFRA detection results with an interval of 30 days, the frequency response curve has a consistent trend with the deepening of the fault degree.The reproducibility of the nanosecond IFRA test was thus verified.

3.4 Working Principle of Power Transformer Winding Based on Nanosecond Pulse

When the frequency is higher (more than 1 kHz), each winding of the transformer can be considered a passive linear dual-port network composed of a distributed parameter such as R, C, and L. After the windings are deformed, the change in the network distribution parameters will cause the pulse response waveform to change, and the transformer winding is deformed by comparison with the test results before and after. This can be injected from the casing end screen, and the output signal can be obtained by the neutral point by a capacitive coupling or a Roche coil, the input and output signals can be obtained after the spectrum analysis is processed. By calculating the correlation coefficient RXY and the mean square difference EXY, the correlation coefficient of curve is determined. Calculate the transfer function of the windings according to the formula (1)–(3), and draw the frequency response.

$$I_i(f) = f_{FFT}(I_i(t)); \tag{1}$$

$$I_o(f) = f_{FFT}(I_o(t)); \tag{2}$$

$$TF = 20 \times 1g\frac{|I_o(f)|}{I_i(f)} \tag{3}$$

In the formula (1)–(3): $I_i(t)$ is an input current time domain signal; $I_i(f)$ is an input current frequency domain signal; $I_o(t)$ is an output current time domain signal; $I_o(f)$ is an output current frequency domain signal; TF is a transfer function.

$$LR_{XY} = \frac{\sum_{i=1}^{n} X_i Y_i - \frac{1}{N} \sum_{i=1}^{n} X_i \sum_{i=1}^{n} Y_i}{\sqrt{\left[\sum_{i=1}^{n} X_i^2 - \frac{1}{N} \left(\sum_{i=1}^{n} X_i\right)^2\right] \left[\sum_{i=1}^{n} Y_i^2 - \frac{1}{N} \left(\sum_{i=1}^{n} Y_i\right)^2\right]}}; \tag{4}$$

In the formula (4)–(6), X_i and $Y_i (i = 1, 2, \ldots, N)$ are the value of two frequency ramming curves before and after the winding deformation R_{XY}. The closer to 1, the better the correlation, the closer E_{XY} closer to 0, the closer the curve. When the shape of the two curves is similar, when the magnitude is different, the order is based on the correlation coefficient as a determination basis.

3.5 Naviosecond Pulse Response Fault Detection Method

Under the action of nanosecond, under high power pulse signal, the winding equivalent circuit generates "parasitic effect" and electromagnetic coupling. Any variations of the windings change the size of the parameters in the circuit model, thereby causing the pulse response of the windings to vary. The transformer windings can measure the excitation signal $U_i(n)$ and the response signal $U_o(n)$ of its N_s point under the action of high-power nanosecond pulse signal, and becomes the amplitude frequency characteristic curve $U_i(k)$ and $U_o(k)$ by fast Fourier transform (FFT). $(n = 0, 1, \ldots, N_{s-1}; 0 \leq k \leq N_{s-1}$; N_s number of sample points for signal acquisition).

Amplitude-frequency characteristic curve expression is input $U_i(k)$ and output $U_o(k)$, as shown in the formula (5) and formula (6).

$$U_i(k) = \sum_{n=0}^{N_{s-1}} U_i(n) \times e^{-j\frac{2\pi}{N_s}kn} \tag{5}$$

$$U_o(k) = \sum_{N=0}^{N_{s-1}} U_o(n) \times e^{-j\frac{2\pi}{N_s}kn} \tag{6}$$

By the formula (7), the transformer winding pulse response curve $H(k)$ is calculated.

$$H(k) = 20 \lg \frac{U_o}{U_i} \tag{7}$$

4 Conclusions

In order to verify the reliability and sensitivity of nanosecond IFRA, this paper compares it with the more mature SFRA method. Under the EE and connection mode II, resonance point basic coincidence of the two methods, along with the degree of fault, the test results of two methods have the same change trend, can be thought of nanosecond IFRA method with reliability test results, there still exists certain differences in the results of two methods, considered to be due to two different kinds of methods of detection device. There is a small difference between the input impedance and output impedance, the specific reasons need further study. According to the industry standard of FRA method in China, three degrees of faults simulated in the experiment were rated, and all three degrees could be evaluated as mild deformation. Therefore, the nanosecond IFRA method was considered to have high sensitivity. The nanosecond IFRA test was repeated at an interval of 30 days, and the consistency of the two test results was high. The repeatability of the nanosecond IFRA method was verified. In addition, compared with SFRA method, the nanosecond IFRA method has higher detection speed and frequency resolution in high frequency band, and the frequency resolution is much lower than that of SFRA method in the frequency range below 100 kHz.

References

[1] Tao S, Lei W, Cheng Z. A Compact Microsecond-Pulse Generator Used for Surface Dielectric Barrier Discharges[J]. IEEE Transactions on Plasma ence, **44(10)**, pp. 1–7, 2016.

[2] Li H, Lukanin A, Tskhe A. Multifunctional generator of high-voltage microsecond pulses[J]. Journal of Electrostatics, **90**, pp. 74–78, 2017.

[3] Puchy V, Kovac F, Petryshynets I. Effect of Microsecond Pulse Laser Modification on Electromagnetic Properties of Grain Oriented Silicon Steel[J]. Materials Science Forum, **891**, pp. 214–218, 2017.

[4] Zhu J, Cui P, Yin G. Pulse-to-pulse alignment based on interference fringes and the second-order temporal coherence function of optical frequency combs for distance measurement[J]. Optics Express, **23(10)**, p. 13069, 2015.
[5] Kozlova E S, Kotlyar V V, Degtyarev S A. Simulation of resonance focusing of a picosecond pulse by a dielectric microcylinder[J]. Computer Optics, **39(1)**, pp. 45–51, 2015.
[6] Xinbing, Cheng, Yongjun. A sub-microsecond-range pulse generator based on anti-resonance network and transmission line transformer.[J]. The Review of scientific instruments, **90(9)**, pp. 94703–94703, 2019.
[7] Fedotov S S, Okhrimchuk A G, Lipatiev A S, et al. 3-bit writing of information in nanoporous glass by a single sub-microsecond burst of femtosecond pulses[J]. Optics Letters, **43(4)**, pp. 851–854, 2018.
[8] Gallmeier F X, Lu W, Riemer B W. Conceptual moderator studies for the Spallation Neutron Source short-pulse second target station[J]. Review of Scientific Instruments, **87(6)**, pp. 1068–1077, 2016.
[9] Jin S, Zhang C, Peng Y. Novel IPOx Architecture for High-Voltage Microsecond Pulse Power Supply Using Energy Efficiency and Stability Model Design Method[J]. IEEE Transactions on Power Electronics, **(99)**, pp. 1–1, 2021.
[10] Sbetti N. Italy and the Olympic Movement after the second World War[J]. IEEE Pulse, **4(4)**, pp. 32–33, 2015.

Biographies

Xinhe Liu, College of electronic systems. Engineer. Graduated from the Northeast Electric Power University in 2010. Worked in Shenzhen Power Supply Bureau Co. Ltd. Her research interests include electrical equipment test, insulation evaluation and fault diagnosis.

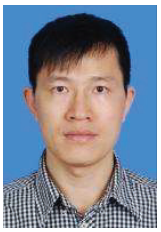

Wenwu Hang, Master of high voltage, Senior Engineer. Graduated from the Wuhan University in 2005. Worked in Shenzhen Power Supply Bureau Co. Ltd. Her research interests include test management of electrical equipment.

Haitao Wu, College of electronic systems, Senior Engineer. Graduated from University of Science and Technology of Chengdu in 1993.Worked in Shenzhen Power Supply Bureau Co. Ltd. Her research interests include power production management and research work.